OPEN

Persistence of envelopes in different CD4$^+$ T-cell subsets in antiretroviral therapy-suppressed people with HIV

Matthew J. Gartner[a,b], Carolin Tumpach[b], Ashanti Dantanarayana[b], Jared Stern[b], Jennifer M. Zerbato[b], J. Judy Chang[b], Thomas A. Angelovich[a,c], Jenny L. Anderson[b], Jori Symons[b], Steve G. Deeks[d], Jacqueline K. Flynn[a,b,e], Sharon R. Lewin[b,f], Melissa J. Churchill[a], Paul R. Gorry[a,*] and Michael Roche[a,b,*]

Objectives: Despite suppressive antiretroviral therapy (ART), HIV can persist in a diverse range of CD4$^+$ T-cell subsets. Through longitudinal *env* sampling from people with HIV (PWH) on ART, we characterized the persistence and phenotypic properties of HIV *envs* over two time-points (T1 and T2).

Methods: Longitudinal blood and lymphoid tissue samples were obtained from eight PWH on suppressive ART. Single genome amplification (SGA) was performed on *env* to understand the genetic diversity and degree of clonal expansions over time. A subset of *envs* were used to generate pseudovirus particles to assess sensitivity to autologous plasma IgG and broadly neutralizing antibodies (bNAbs).

Results: Identical *env* sequences indicating clonal expansion persisted between T1 and T2 and within multiple T-cell subsets. At both time-points, CXCR4-tropic (X4) Envs were more prevalent in naive and central memory cells; the proportion of X4 Envs did not significantly change in each subset between T1 and T2. Autologous purified plasma IgG showed variable neutralization of Envs, with no significant difference in neutralization between R5 and X4 Envs. X4 Envs were more sensitive to neutralization with clinical bNAbs, with CD4-binding site bNAbs demonstrating high breadth and potency against Envs.

Conclusion: Our data suggest the viral reservoir in PWH on ART was predominantly maintained over time through proliferation and potentially differentiation of infected cells. We found the humoral immune response to Envs within the latent reservoir was variable between PWH. Finally, we identified coreceptor usage can influence bNAb sensitivity and may need to be considered for future bNAb immunotherapy approaches.

AIDS 2023, **37**:247–257

Keywords: CCR5, CXCR4, HIV tropism, neutralization, reservoir, T-cell subsets

[a]School of Health and Biomedical Sciences, RMIT University, [b]The Peter Doherty Institute for Infection and Immunity, University of Melbourne and Royal Melbourne Hospital, [c]Life Sciences, Burnet Institute, Melbourne, Victoria, Australia, [d]School of Medicine, University of California San Francisco, San Francisco, California, USA, [e]School of Clinical Sciences, Monash University, and [f]Department of Infectious Diseases, Monash University and Alfred Hospital, Melbourne, Victoria, Australia.

Correspondence to Paul R. Gorry, and Michael Roche, School of Health and Biomedical Sciences, RMIT University, Melbourne, VIC, Australia.

E-mail: Paul.gorry@rmit.edu.au and Michael.roche@rmit.edu.au

* P.R.G. and M.R. are co-corresponding authors.

Received: 30 November 2020; revised: 28 October 2022; accepted: 2 November 2022.

DOI:10.1097/QAD.0000000000003424

ISSN 0269-9370

Background

A major barrier to HIV-1 cure is the establishment and persistence of latently infected cells [1]; these cells are predominantly maintained in virally suppressed people with HIV-1 (PWH) through cellular proliferation [2–4] via homeostatic [5], antigen-mediated [6,7], or integration site-induced mechanisms [8,9]. A proportion of clonally expanded cells are transcriptionally active during antiretroviral therapy (ART) [10], and a smaller proportion can generate replication-competent virus [2,3,6,11,12]; clonal cells can contribute to viral rebound following ART interruption [13]. In a cross-sectional study of eight PWH on long-term suppressive ART, we identified identical proviral sequences within different $CD4^+$ T-cell subsets, suggesting differentiation of subsets may contribute to reservoir persistence [14]. Whether this persists over time remains unknown.

Proviral DNA is present in naive, stem cell memory, central memory, transitional memory, effector memory, and terminally differentiated $CD4^+$ T cells in PWH on ART [5,14–16]. These subsets demonstrate similar properties in the induction of infectious proviruses following stimulation, suggesting that each subset may contribute to viral rebound [17]. Furthermore, these subsets differ in activation status [18] and expression of coreceptors for viral entry [19,20], with less differentiated cells expressing higher CXCR4 levels and more differentiated subsets expressing higher CCR5 levels [19,20]. Coreceptor tropism may influence the establishment of the reservoir in diverse subsets [14]. We have previously observed CXCR4-tropic (X4) *envelopes* (*envs*) predominantly in naive and central memory cells in PWH on suppressive ART. Whether these X4 Envs persist in naive and central memory cells over time or become more distributed across transitional memory and effector memory subsets through differentiation is unclear.

Broadly neutralizing antibodies (bNAbs) show potential activity in clearing the reservoir and/or controlling viral replication on ART when used in combination with toll-like receptor-7 agonists, as recently demonstrated in an animal model [21]; bNAbs have also delayed viral rebound in some individuals treated with ART early after infection and may enhance HIV-specific T-cell immunity [22,23]. Whether coreceptor usage diversity in the reservoir affects sensitivity to bNAbs or autologous antibodies remains unclear. Bertagnolli *et al.* [24] found that a variable fraction of replication-competent proviruses were susceptible to neutralization with IgG isolated from autologous plasma samples, suggesting reservoir diversity may present a barrier to the autologous antibody response. Furthermore, virus sensitivity to bNAbs has been shown to differ between R5 and X4 Envs and may pose challenges for bNAb-based therapeutic strategies [25].

In this study, we investigated the mechanisms driving viral persistence during suppressive ART by tracking the movement of proviruses through different $CD4^+$ T-cell subsets by coreceptor usage. We hypothesized that the reservoir is constantly being replenished from a naive or central memory population, and that over time there would be an enrichment within the effector memory population of viruses. Additionally, we assessed the change in autologous humoral antibody response over time during suppressive ART and whether coreceptor usage influences virus sensitivity to autologous plasma. Finally, we evaluated the sensitivity of Envs from PWH on suppressive ART to bNAbs currently being evaluated clinically, and whether Env coreceptor usage influences virus sensitivity to bNAbs.

Methods

Study participants

Biospecimens were obtained at two time-points (2–4 years between sampling) from eight virally suppressed PWH (defined by viral load <40 copies/ml, $CD4^+$ T-cell counts >350 cells/μl for >2 years) recruited by the University of California San Francisco [26]. Rectal tissue and lymph node biopsies were performed on six and three participants at time-point 1 (T1), respectively. Pre-ART plasma was obtained from two participants. Peripheral blood mononuclear cells (PBMCs) were obtained at all time-points including a third time-point for participant 7, 60 weeks after time-point 2 (T2).

Single genome amplification and sequence analysis of isolated T-cell subsets

Briefly, $CD4^+$ T-cell subsets [including terminally differentiated cells ($CD4^+CD45RA^+CD27^-CCR7^-$) for some donors (subject to cell numbers) were isolated from PBMCs by fluorescence-activated cell sorting, as previously described [14]. Single genome amplification (SGA) of full-length *envs* and Sanger sequencing was performed on genomic DNA (gDNA) from isolated T-cell subsets, as previously described [14]. SGA was performed on lymph node, rectal tissue and pre-ART plasma in our previous study [14].

Phylogenetic analysis

Neighbour-joining trees were generated using MEGA7 [27] and edited using FigTree v1.4.3 (available at http://tree.bio.ed.ac.uk/software/figtree/), with evolutionary distances calculated using the maximum composite likelihood method [28]. Maximum likelihood phylogenies were generated for each participant using MEGA7 [27], using the general time-reversible nucleotide substitution model [29] incorporating gamma-distributed rate variation among sites and 100 bootstrap replicates were generated for variance estimation.

Compartmentalization analysis

Panmixia tests were run using 10 000 permutations (http://wwwabi.snv.jussieu.fr/public/mpweb) and P less than 0.001 was considered significant [30]. Simmond's artificial intelligence tests were conducted using Hypothesis Testing using Phylogenies (HyPhy) with 1000 bootstrap trees and 10 random relabellings per sample [31]. Artificial intelligence values of 1 indicate no difference in genetic compartmentalization, while artificial intelligence values closer to 0 indicate genetic compartmentalization between sequences and were only considered significant if bootstrap values were greater than 0.95.

Production and titration of Env-pseudotyped reporter viruses

Env-pseudotyped luciferase reporter viruses were produced by transfection of 293T cells with pcDNA3.1-Env and pNL4.3e-luc plasmids and titrated in JC53 cells, as previously described [14].

Isolation of plasma IgG

Autologous IgG antibodies were purified from plasma samples taken from two different time-points (one contemporaneous to the first env sampling timepoint, the second 2–3 years later. Briefly, diluted plasma was applied to Melon IgG Spin Purification Gel (Thermo Scientific, Waltham, Massachusetts, USA) and IgG purified following the manufacturer's instructions. The resulting eluates were buffer exchanged in PBS twice using Amicon Ultra-15 (Millipore, Burlington, Massachusetts, USA) spin filters with 100 kDa molecular weight cut-off.

Neutralization assays

One hundred $TCID_{50}$ of Env-pseudotyped luciferase reporter virus was incubated with five-fold serial dilutions of antibody (20 μg/ml to 0.00064 μg/ml) for 1 h at 37 °C or three-fold serial dilutions of purified plasma IgG (300–3.7 μg/ml) for 90 min at 37 °C. JC53 cells in 96-well plates were inoculated with virus/antibody mixtures and incubated overnight at 37 °C before culture media was replaced and incubated for a further 48 h at 37 °C. Virus infectivity was measured by luciferase activity in cell lysates (Promega, Madison, Wisconsin, USA) as per manufacturer's protocol relative to negative controls incubated with culture medium alone. Neutralization activity was determined by percentage inhibition calculated as 100% − (luciferase units with antibody/luciferase units without antibody). Data were fitted with a nonlinear function, and 50% inhibitory concentrations (IC_{50}) were calculated by least squares regression analysis [32–34].

Statistical analysis

All statistical analyses were performed using GraphPad Prism v7.0; (GraphPad Software, San Diego, California, USA). Single comparisons between groups were assessed by nonparametric Mann–Whitney or Wilcoxon signed rank sum tests and multiple comparisons were assessed by Kruskal–Wallis or Friedman test with Dunn's post hoc test. P values less than 0.05 are statistically significant: $^{*}P$ less than 0.05; $^{**}P$ less than 0.01; $^{***}P$ less than 0.001; $^{****}P$ less than 0.0001.

Results

Amplification and sequencing of HIV *envs*

To investigate the mechanisms sustaining the peripheral blood reservoir of PWH on ART, we analysed viral evolution over time in $CD4^+$ T-cell subsets from eight PWH via SGA and Sanger sequencing of *env* sequences [26,35–37]. We have previously published a cross-sectional analysis of HIV-1 *envs* from these participants [14]; *env* sequences generated in our previous study are referred to herein as time-point 1 (T1). All participants maintained an undetectable plasma viral load on ART for at least 2 years (Supplementary Table 1, http://links.lww.com/QAD/C711). In this study, we resampled PBMCs from participants 2–4 years after T1 [referred to as time-point 2 (T2)]; cells were sorted into $CD4^+$ T-cell subsets: naive, central memory, transitional memory, effector memory and terminally differentiated. $CD4^+$ T-cell subsets were used for DNA purification and SGA was performed to amplify *envs*; Sanger sequencing was performed on the V1–V5 region of *env* sequences. Additionally, a third time-point was collected for participant 3, 60 weeks after T2 and used to generate *env* sequences by SGA.

No evidence for ongoing residual replication in people with HIV on antiretroviral therapy

We generated and sequenced 1123 *env* sequences (Supplementary Table 2, http://links.lww.com/QAD/C711). A neighbour-joining tree of showed no contamination of sequences across participants (Supplementary Figure 1, http://links.lww.com/QAD/C711). Maximum-likelihood trees were generated for each participant and showed intermingling of sequences across time-points and different $CD4^+$ T-cell subsets (Fig. 1 and Supplementary Figure 2, http://links.lww.com/QAD/C711). Additionally, we observed no change in intra-participant sequence diversity between T1 and T2 when identical sequences were excluded (Fig. 2a). Furthermore, no changes were seen in the sequence diversity between $CD4^+$ T-cell subsets over time (Fig. 2b). Panmixia genetic compartmentalization tests were also performed (Supplementary Table 3, http://links.lww.com/QAD/C711). We saw compartmentalization between T1 and T2 in participants 5–7 ($P = 0.0004$, 0.0001 and 0.0003, respectively), and between pre-therapy plasma vs. T1 and T2 in participant 2 ($P < 0.0001$ and $P = 0.0003$, respectively). However, these data were not statistically significant when identical sequences were excluded from each time-point. An additional compartmentalization test (Simmonds AI) found no evidence of compartmentalization of sequences between T1 and T2

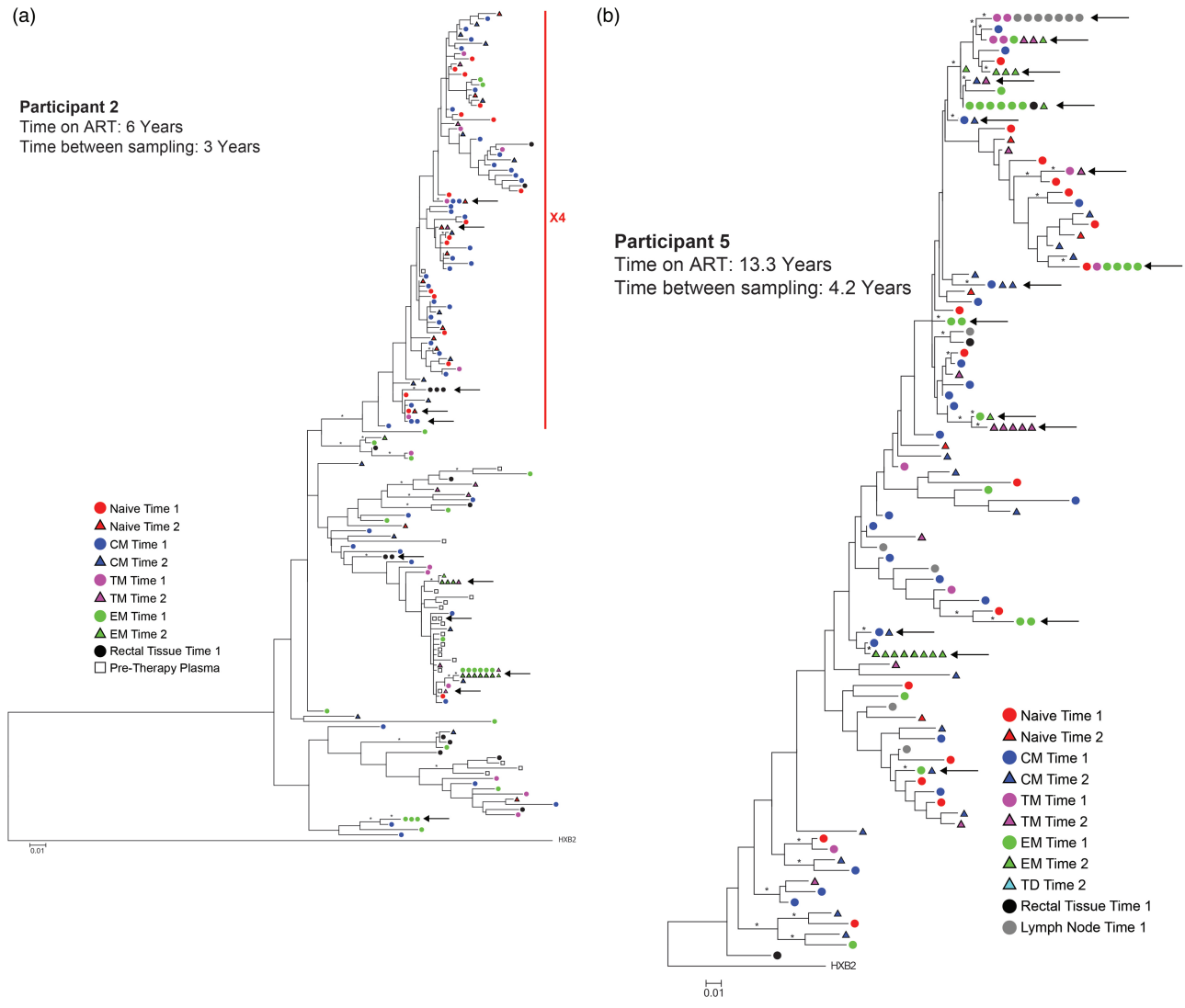

Fig. 1. Phylogenetic analysis of *env* sequences. Maximum likelihood trees were generated for *env* sequences isolated from blood [naive, central memory (CM), transitional memory (TM), effector memory (EM) and terminally differentiated (TD)], rectal tissue (total $CD4^+$), lymph node (total $CD4^+$) and plasma collected from participants 2 (a) and 5 (b). Sequences obtained from pre-therapy are shown as squares, time point 1 derived *envs* are circles and time point 2 derived *envs* are triangles, with the colour of each shape referring to the cell subset. Black arrows indicate clusters of identical sequences. Red lines with 'X4' indicate CXCR4-using *env* clusters (determined by Geno2Pheno score). Asterisks represent bootstrap values above 70 and the scale indicates the number of nucleotide substitutions per site. These participants were selected as they provide the best representation of the conclusions drawn from these data. Data for other participants are shown in Supplementary Figure 2, http://links.lww.com/QAD/C711.

(Supplementary Table 3, http://links.lww.com/QAD/C711). Overall, sequence diversity analysis and genetic compartmentalization testing showed minimal evidence of the reservoir persisting through sustained ongoing cycles of viral replication between time-points.

Increase in identical sequences hints at clonal expansion maintaining the reservoir

Within all eight phylogenetic trees (Fig. 1 and Supplementary Figure 2, http://links.lww.com/QAD/C711), we observed clusters of identical sequences, suggestive of clonal expansion of latently infected cells. At T2, we found that the percentage of identical sequences was higher in more differentiated T-cell subsets, especially in effector memory cells when compared with naive and central memory ($P = 0.0029$ and 0.0033, respectively; Fig. 2c). This is consistent with our previous cross-sectional analysis of T1, which found a higher degree of clonal expansion in effector memory compared with naive and central memory [14]. No significant differences were seen in identical sequences within each subset between T1 and T2 (Fig. 2d and Supplementary Table 4, http://links.lww.com/QAD/C711). Furthermore, 40% of clonally expanded sequences persisted across the time-points sampled (data not shown),

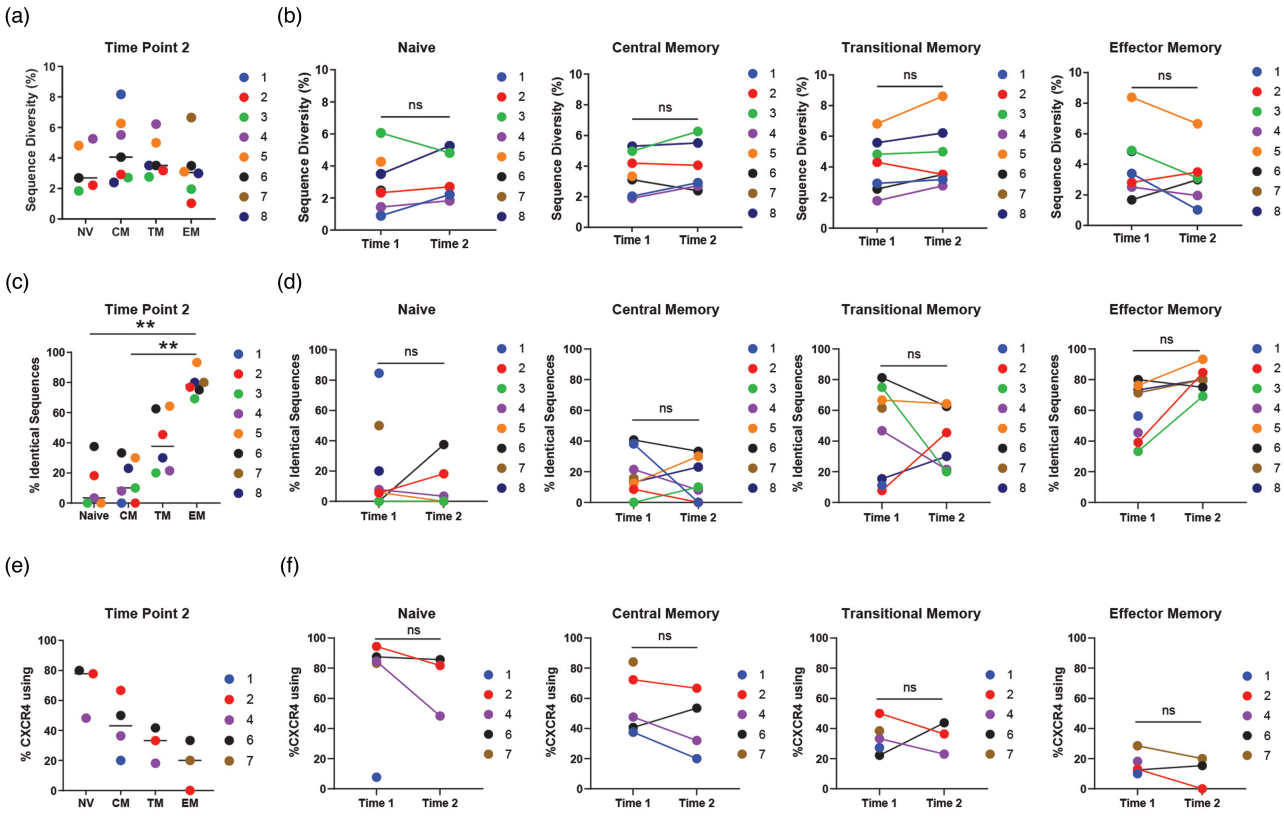

Fig. 2. Identical sequences indicate clonal expansion maintains the reservoir over time. (a) Identical sequences as a percentage of total sequences were plotted for each participant stratified by $CD4^+$ T-cell subset at time-point 2 [T2, note: corresponding data for time-point 1 (T1) has previously been reported [14]]. Each symbol represents a participant while the lines represent the median of identical sequences within each $CD4^+$ T-cell subset. (b) Change in the percentage of identical sequences within each subset [naive, central memory (CM), transitional memory (TM), and effector memory (EM)] between T1 and T2. Each participant is shown in a different colour circle with black lines linking T1 and T2 data points for each participant. (c) Average pairwise distance of Env sequences for each participant stratified by $CD4^+$ T-cell subset at time-point 2 (note: this data for time-point 1 has previously been reported [14]). Each symbol represents a participant while the lines represent the median of identical sequences within each $CD4^+$ T-cell subset. (d) Change in average pairwise distance of Env sequences within each subset [naive, central memory, transitional memory and effector memory (EM)] between T1 and T2. Each participant is shown in a different colour circle with black lines linking T1 and T2 data points for each participant. (e) Percentage of CXCR4-using Envs for each participant stratified by $CD4^+$ T-cell subset at time-point 2 (note: this data for time-point 1 has previously been reported [14]). Each symbol represents a participant while the lines represent the median of CXCR4-using Envs within each $CD4^+$ T-cell subset. (f) Change in CXCR4-using Env sequences within each subset (naive, central memory, transitional memory, and effector memory) between T1 and T2. Each participant is shown in a different colour circle with black lines linking T1 and T2 data points for each participant. Statistical comparisons for (a), (c) and (e) used the Kruskal–Wallis test with Dunn's post hoc test for multiple comparisons and for (b), (d) and (f) were conducted using the Wilcoxon signed sum rank test. $^*P < 0.05$; $^{**}P < 0.01$; $^{***}P < 0.001$, $^{****}P < 0.0001$.

with one expansion detected in effector memory cells at all three time-points from participant 7 (Supplementary Figure 2e, http://links.lww.com/QAD/C711). Additionally, we observed 45% of identical sequences were present in more than one subset, suggestive of cellular differentiation maintaining latently infected cells. Overall, our data suggests that proliferation and possibly differentiation of latently infected cells maintains the reservoir in PWH on suppressive ART.

Envelope coreceptor usage

Next, we sought to use coreceptor usage to track the movement of proviruses through different T-cell subsets over time. Phylogenetic trees demonstrated compartmentalization of X4 *envs* from R5 *envs* (Fig. 1 and Supplementary Figure 2, http://links.lww.com/QAD/C711). Identical sequences were removed for the analysis of X4 Env distribution amongst $CD4^+$ T-cell subsets. X4 *envs* were found predominantly within less differentiated cells (naive and central memory, Fig. 2e) at T2; however, given the low sample size per subset ($n = 3–5$), the differences in X4 Envs between subsets were not statistically significant. Surprisingly, X4 prevalence remained consistent across each $CD4^+$ T-cell subset between the two time-points sampled (Fig. 2f).

Autologous plasma IgG neutralization of Env-pseudoviruses

We next sought to determine the sensitivity of reservoir Envs to autologous neutralizing antibodies (IgG). Single-round Env pseudoviruses were generated using Envs sampled from four participants (P1, P2, P5 and P6) from T1. Neutralization assays were performed with Envs from T1 and serial dilutions of purified IgG from autologous contemporaneous and follow-up plasma samples obtained 3 years later (Supplementary Table 5, http://links.lww.com/QAD/C711); follow-up plasma IgG sampling did not coincide with T2 PBMC sampling for Env analysis. Inhibition curves were created and maximum percentage inhibition (MPI) and area under the neutralization curve (AUC) were calculated [38,39].

We found neutralization of the control viruses NL4.3 (CXCR4-using) and AD8 (CCR5-using) was variable with purified IgG from the four participants (Supplementary Figure 3a, http://links.lww.com/QAD/C711). Moreover, we did not see substantial differences in the neutralization curves of control viruses when comparing contemporaneous and follow-up IgG samples (Supplementary Figure 3a, http://links.lww.com/QAD/C711). Similarly, participant-derived T1 Env-pseudoviruses demonstrated variable neutralization sensitivity to contemporaneous and follow-up IgG (Supplementary Figure 3, http://links.lww.com/QAD/C711). We observed that P5 showed the poorest neutralization of contemporaneous Envs as well as NL4.3 and AD8 (Supplementary Figure 3, http://links.lww.com/QAD/C711). IC_{50} values for 18/22 Envs were above the limit of detection (>300 μg/ml) for both contemporaneous and follow-up IgG samples, with Envs from P2 and P6 recording detectable IC_{50} against autologous IgG samples (Supplementary Figure 3, http://links.lww.com/QAD/C711).

Given that most autologous IgG samples demonstrated IC_{50} values above the limit of detection, we analysed AUC and MPI (at 300 μg/ml) to understand the antibody response during suppressive ART. We found a significant increase in the AUC for follow-up IgG samples compared with contemporaneous IgG ($P = 0.0391$; Fig. 3a). When these data were stratified by participant, there were marginal decreases in AUC at follow-up compared with contemporaneous IgG for P2 and P6 and slight increases for P1 and P5 (Fig. 3b); none of these differences were statistically significant.

Analysis of the MPI at 300 μg/ml of purified autologous IgG against Envs showed a small statistically significant increase with follow-up compared with contemporaneous IgG ($P = 0.0301$; Fig. 3c). When stratified by participant, we found no significant differences in MPI between time-points within each participant, suggesting no improvement in antibody neutralization of Envs over time on suppressive ART (Fig. 3d). In addition, we stratified the MPI data within each participant by Env coreceptor usage; this analysis did not show any significantly significant differences in the neutralization of R5- and X4-using Envs by autologous contemporaneous or follow-up plasma for P1, P2 and P6 when the data were combined or stratified by participant (Fig. 3e and f). Although our collated AUC and MPI data showed small increases in autologous plasma neutralizing of Envs over time, participant-specific data showed no improvement in the host antibody response against Envs.

Env-pseudovirus neutralizing sensitivity to broadly neutralizing antibodies

BNAbs represent a promising strategy for therapeutic interventions in HIV-1 treatment and cure strategies. However, whether coreceptor usage influences sensitivity to clinical bNAbs and these bNAbs neutralize the whole repertoire of Envs in the reservoir is unclear. We assessed the ability of five bNAbs to neutralize 27 T1 Env-pseudoviruses from four participants (P1, P2, P4 and P6). T1 Envs were derived from naive ($n = 7$), central memory ($n = 4$), transitional memory ($n = 8$) and effector memory ($n = 8$) cells (R5: $n = 18$, dual: $n = 9$ and X4: $n = 1$). We used two CD4-binding site (CD4bs) antibodies 3BNC117 and VRC01, the V3-glycan targeting antibodies 10-1074 and PGT121, and the membrane proximal external region (MPER) antibody 10E8. Neutralization assays were performed using the tri-specific antibody N6/PGDM1400x10E8 against a subset of the virus panel ($n = 8$).

All viruses tested were sensitive to 3BNC117, VRC01 and N6/PGDM1400x10E8 with median IC_{50} values of 0.05, 0.19 and 0.07 μg/ml, respectively (Fig. 4a and Supplementary Figure 4, http://links.lww.com/QAD/C711). Investigation of V3-targeting bNAbs revealed 7 of 27 (26%) and 10 of 27 (37%) pseudoviruses were resistant to 10-1074 and PGT121 respectively, with median IC_{50} values for sensitive viruses of 0.077 and 0.079 μg/ml (Fig. 4a and Supplementary Figure 4b and c, http://links.lww.com/QAD/C711). Furthermore, 1 of 27 (3%) pseudoviruses was resistant to 10E8, and the median IC_{50} for viruses sensitive to 10E8 was 0.05 μg/ml (Fig. 4a and Supplementary Figure 4d, http://links.lww.com/QAD/C711). After stratifying neutralizing sensitivity by coreceptor usage, dual-tropic Envs were more sensitive to neutralization by VRC01 and 10E8 compared with R5 Envs ($P = 0.03$ and $P = 0.006$ respectively, Fig. 4b). Furthermore, dual-tropic Envs were more likely to be resistant to PGT121 and less likely to be resistant to 10-1074 than R5 Envs (Fig. 4b). Interestingly, dual-tropic viruses that were sensitive to PGT121 demonstrated lower IC_{50} values compared with sensitive R5 Envs ($P = 0.04$, Fig. 4b).

We observed no differences in IC_{50} values for the bNAbs tested when Envs were stratified by subset of origin (Fig. 4c). Neutralizing sensitivity appeared to be participant-specific for 10-1074 and PGT121 (Fig. 4d), with Envs from participant 6 demonstrating a high rate of resistance to 10-1074 (6/8) and PGT121 (5/8). Moreover,

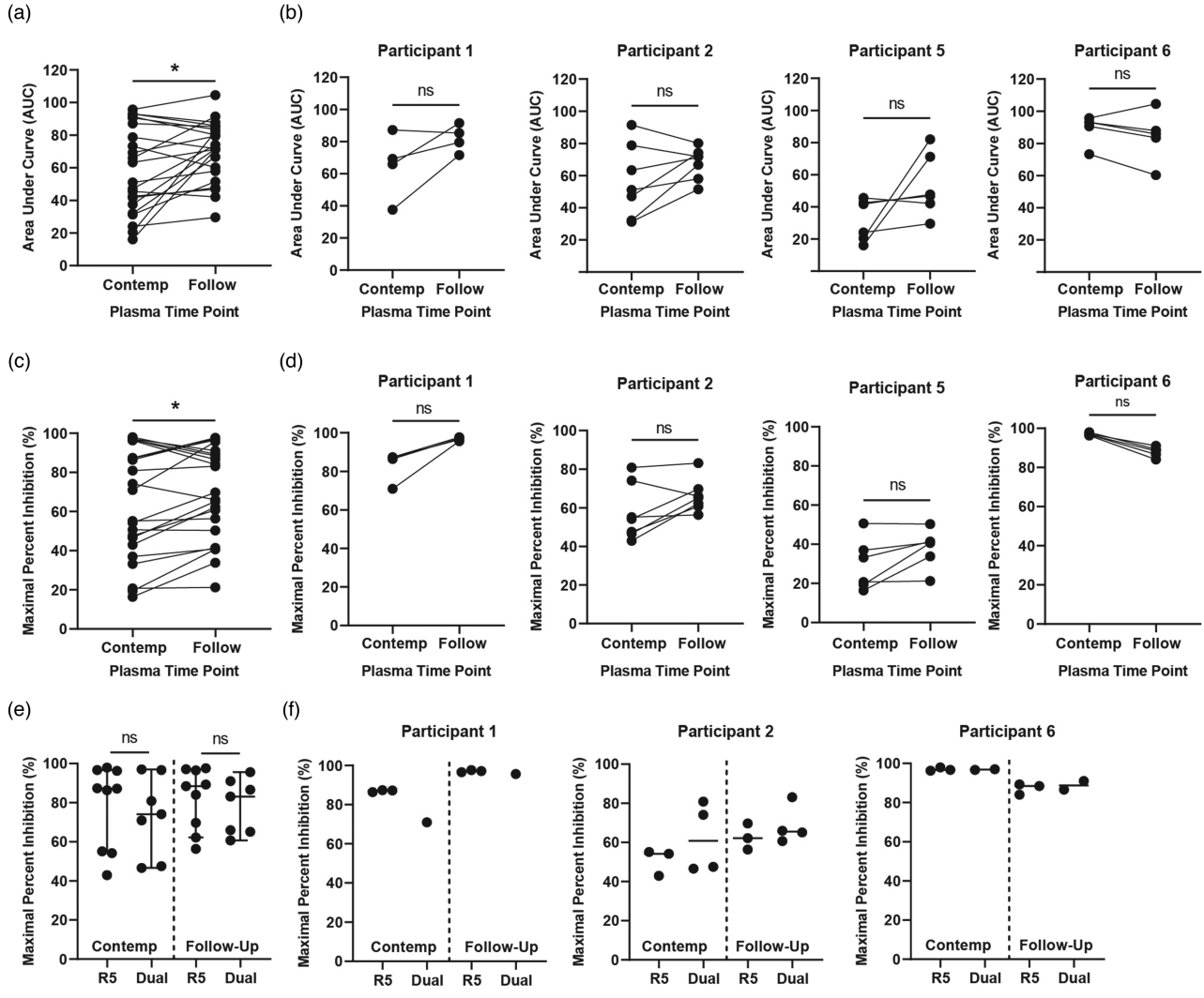

Fig. 3. Neutralization of T1 Envs by autologous IgG samples. (a) Neutralization sensitivity of T1 Env-pseudoviruses against autologous contemporaneous ('Contemp') and follow-up ('Follow') plasma IgG represented as the area under the inhibition curve (AUC). (b) Neutralization sensitivity data represented as AUC stratified by participant (P1, P2, P5 and P6). (c) Neutralization sensitivity of T1 Env-pseudoviruses against autologous contemporaneous and follow-up plasma IgG represented as the maximal percentage inhibition (MPI) at an IgG concentration of 300 μg/ml. (d) MPI data stratified by participant (P1, P2, P5 and P6). (e) MPI of T1 Envs to contemporaneous and follow-up IgG stratified by CCR5-using (R5) and dual-tropic (dual) Envs. (f) Neutralizing sensitivity of T1 Envs grouped by coreceptor usage stratified by participant (P1, P2 and P6). Each dot represents one T1 Env against purified IgG averaged over two independent experiments. Lines link T1 Env data for contemporaneous and follow-up IgG. Statistical comparisons for (a)–(d) used the Wilcoxon signed sum rank test and (e)–(f) used the Mann–Whitney *U* test. $^{*}P < 0.05$; $^{**}P < 0.01$; $^{***}P < 0.001$, $^{****}P < 0.0001$.

N6/PGDM1400x10E8 effectively neutralized viruses that were resistant to 10-1074 and PGT121 (Fig. 4e and Supplementary Figure 4g, http://links.lww.com/QAD/C711). Overall, our neutralization assays suggest that dual-tropic Envs demonstrated an increased sensitivity to bNAbs targeting diverse epitopes.

Discussion

In this study, we utilized *env* genotypic and phenotypic properties to gain insights into the maintenance of the reservoir in different $CD4^{+}$ T-cell subsets in PWH on suppressive ART. Phylogenetic analysis of *env* sequences from two time-points of ART-suppressed PWH did not reflect viral evolution suggestive of ongoing replication, consistent with previous studies [30,40,41]. Instead, proliferation and differentiation of latently infected cells was more likely the main driver of reservoir persistence in the participants studied. X4 *envs* persisted in naive and central memory subsets but did not increase in more differentiated subsets over time. Pseudoviruses generated with T1 Envs demonstrated variable sensitives to contemporaneous serum IgG antibodies. Moreover, no

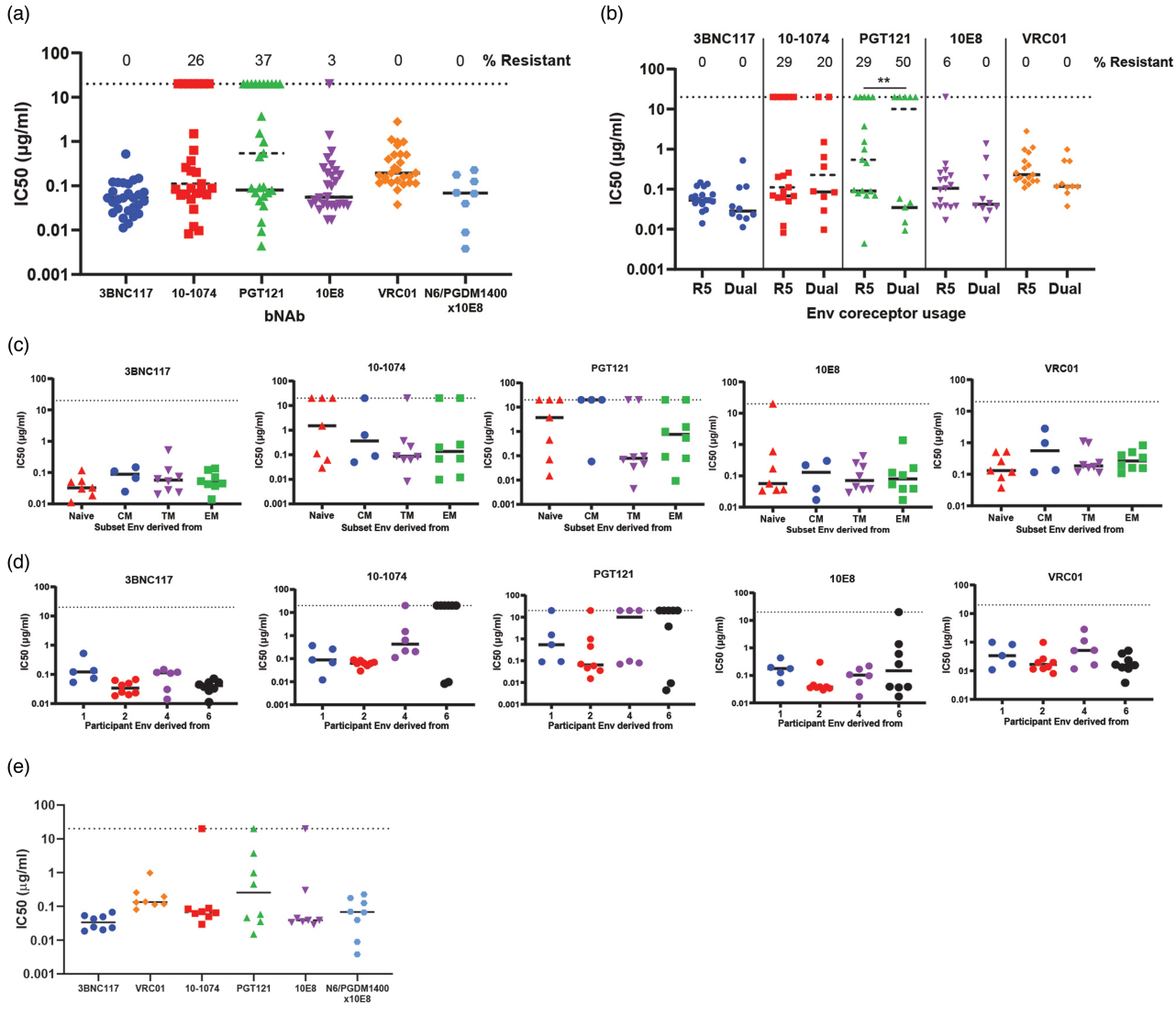

Fig. 4. Neutralization profiles with different clinical broadly neutralizing antibodies are similar between viruses with different coreceptor usage and subset of origin. Scatter plots representing the IC_{50} of (a) all pseudoviruses and (b) stratified by virus coreceptor usage (CCR5-tropic: R5 and dual-tropic: dual). Each virus is represented by an individual dot, the dotted line at $y = 20$ represents the limit of detection, dotted lines represent the median IC_{50} titre of all viruses in that group and solid lines represent the median IC_{50} titre of sensitive viruses. (c) Neutralizing sensitivity of Env-pseudoviruses represented as IC_{50} to bNAbs stratified by $CD4^+$ T-cell subset (naive, central memory, transitional memory and effector memory). Each virus is presented by an individual dot, black lines represent the median within each group and the dotted line at $y = 20$ represents the upper limit of detection. (d) Neutralizing sensitivity of Env-pseudoviruses represented as IC_{50} to bNAbs stratified by participant (P1, P2, P4 and P6). Each virus is presented by an individual dot, black lines represent the median within each group and the dotted line at $y = 20$ represents the upper limit of detection. (e) IC_{50} of Env-pseudoviruses that were tested against N6/PGDM1400x10E8 against 3BNC117, 10-1074, PGT121, 10E8 and VRC01. Each virus is presented by an individual dot, black lines represent the median within each group and the dotted line at $y = 20$ represents the upper limit of detection. Statistical comparisons were performed using the Mann–Whitney test. $^*P < 0.05$; $^{**}P < 0.01$; $^{***}P < 0.001$, $^{****}P < 0.0001$.

participants demonstrated a significant improvement in IgG potency with follow-up IgG antibodies. Assessment of neutralizing sensitivity of Envs to a panel of clinical bNAbs showed dual-tropic viruses were often more sensitive to neutralization than R5 Envs.

Identical sequences increased over time in six of eight participants investigated, consistent with previous studies showing an increase in clonality over time in PWH on suppressive ART [42,43]. Furthermore, effector memory cells contained more identical sequences and expansions were typically larger than other subsets. Additionally, we observed that 45% of identical sequences were shared across multiple T-cell subsets. These data support our previous study and suggest that clones can undergo differentiation, probably through an antigen-driven

mechanism [6,14]. Previous studies have found that T cells can proliferate in response to phytohemagglutinin, anti-CD3/CD28, or IL-7 without producing infectious virus [6,11]. Furthermore, Wang *et al.* [6] reported that predominant viral clonal populations waxed and waned over time during suppressive ART, suggesting that the expansion and contraction of clones was controlled by cognate antigen. Whether the differentiation of cells in an antigen-driven manner can lead to the generation of new clones without virus production remains unknown. Furthermore, the ability of clones to differentiate, survive the 'contraction' phase of an immune response and remain latent over long periods of time warrants further investigation.

Our hypothesis was that proviruses found within naive and central memory cells would replenish the reservoir in effector memory cells over time through cellular differentiation. The emergence of X4 *envs* in five of the eight participants in this study provided a unique opportunity to track this phenomenon. Contrary to our hypothesis, the percentage of *envs* predicted to be X4 did not significantly change in each T-cell subset over time. This observation may be influenced by the reduced sampling depth of participants at T2 compared with T1. Given the low contribution of naive cells to the total reservoir [5], this phenomenon may take a longer period of time than our sampling allowed for. To our knowledge, this is the first study to longitudinally track the movement of proviruses through different $CD4^+$ T-cell subsets by coreceptor usage in PWH on suppressive ART.

Untreated HIV infection is characterized by an evolutionary arms-race between the humoral immune response and the rapid evolutionary escape of Envs from antibody responses [44–46]. Studies in untreated PWH have demonstrated that serum-derived antibodies effectively neutralize previous circulating Envs but poorly neutralize contemporaneous Envs [44–46]. We aimed to understand the landscape of immunological pressure on the latent reservoir during suppressive ART. Our analysis of Env sensitivity to autologous contemporary purified plasma IgG samples showed that antibody responses vary widely in their potency to neutralize autologous Envs. These findings are consistent with findings from Bertagnolli *et al.* [24] and Wilson *et al.* [47] both of which studied the sensitivity of replication-competent Envs to autologous plasma IgG. We reasoned that the lack of viral replication and opportunity for antigenic change during suppressive ART would lead to minimal change in antibody responses to Envs within the reservoir. Indeed, our neutralization assays did not show an improvement in antibody responses to autologous T1 Envs over time.

Neutralization assays showed that 3BNC117, VRC01, 10E8 and N6/PGDM1400x10E8 demonstrated notable breadth against our panel of 27 Env-pseudoviruses, with dual-tropic strains demonstrating increased neutralizing sensitivity, consistent with previous findings [25,48]. In contrast, Registre *et al.* [25] found that Envs that exclusively use CXCR4 were less sensitive to PGT121 and 10-1074 than R5 Envs. These studies together with our data suggest that dual-tropic viruses may be more susceptible to neutralization through the exposure of key neutralization epitopes during the evolutionary switch from R5-to-X4 usage, and that evolution of Envs that exclusively use CXCR4 may re-mask these key epitopes. Our neutralization assay data was consistent with a recent study that assessed a panel of 14 bNAbs against viruses outgrown from PBMCs of PWH on suppressive ART, which showed 3BNC117 demonstrated the highest breadth and potency [49].

Our study contains some limitations including that our sampling depth at T2 was limited (<4 *envs* per subset) for several participants, and we were unable to quantify cell-associated HIV DNA or RNA in each subset, which may limit our interpretation of the sequencing data. Additionally, our sub-genomic sequencing of the V1–V5 of *env* does not discriminate between intact and defective proviruses [50,51]. Although given the propensity of *env* defects in defective proviruses, our sequencing approach likely enriches for intact proviruses [14]. Another limitation of this work is that our neutralization assay using JC53 cells may overestimate neutralizing sensitivity compared to infectious molecular clones produced in 293T or PBMCs and viruses outgrown from PBMCs [52,53].

In conclusion, overall, this study suggests that cellular proliferation and differentiation drive the persistence of latently infected cells within $CD4^+$ T cells of PWH on suppressive ART. Despite this finding, X4 *envs* did not increase in more differentiated subsets at T2 as hypothesized. We found the humoral response during long-term suppressive ART varies widely in ability to neutralize contemporaneous Envs and was not influenced by Env coreceptor usage. Finally, we showed differential sensitivities of R5 and X4-using Envs to clinically relevant bNAbs, which may be an important consideration for future bNAb-based therapies.

Acknowledgements

We acknowledge the Melbourne Cytometry Platform (Doherty Institute node) for provision of flow cytometry services. We thank D. Kabat for providing JC53 cells. TZM-bl cells (Catalogue #8129), 3BNC117 (Catalogue #12474), VRC01 (Catalogue # 12033), 10–1074 (Catalogue #12477), PGT121 (Catalogue #12343), 10E8 (Catalogue #12294) and N6/PGDM1400x10E8 (Catalogue #13390) were obtained through the AIDS Research and Reference Reagent Program, Division of AIDS, NIAID, NIH.

Funding: This study was supported by a grant from amfAR, The Foundation for AIDS Research (109114-57-RGRL) to M.R. M.G. was supported by an Australian Research Training Program Award from RMIT University. J.K.F. and T.A.A. were supported by RMIT Vice Chancellor Postdoctoral Fellowships. M. R. was supported by an NHMRC Early Career Fellowship. S.R.L. is an NHMRC practitioner fellow and is supported by the National Institutes of Health (NIH) Delaney AIDS Research Enterprise (DARE U19 AI096109 and UM1 AI126611-01).

Author's contributions: S.R.L. and M.R. conceptualized the study. M.J.G., C.T. and M.R. performed single genome amplification and *env* sequencing experiments. M.J.G. and M.R. analysed *env* sequences and performed phylogenetic analysis. M.J.G., C.T., J.M.Z. and M.R. performed in-vitro pseudovirus infection assays. A.D. and J.S. processed clinical samples. J.J.C. and T.A.A. provided flow cytometry and statistics advice, respectively. S.G.D. provided clinical samples for the study. M.J.G. and M.R. wrote the manuscript. All authors read and edited the manuscript.

Data availability: *Env* sequences generated or used in this study have been deposited into GenBank under the accession numbers MK465705 to MK466337 and MW017710.1 to MW018129.1.

Conflicts of interest

There are no conflicts of interest.

Presented in part: mHIVE World AIDS Day, the Peter Doherty Institute, Melbourne, Australia, 29th November 2019; Keystone Conference on Functional Cures and Eradicating HIV, Whistler, Canada, 24th to 28th March, 2019.

References

1. Finzi D, Blankson J, Siliciano JD, Margolick JB, Chadwick K, Pierson T, *et al*. **Latent infection of CD4$^+$ T cells provides a mechanism for lifelong persistence of HIV-1, even in patients on effective combination therapy.** *Nat Med* 1999; **5**:512–517.
2. Bui JK, Sobolewski MD, Keele BF, Spindler J, Musick A, Wiegand A, *et al*. **Proviruses with identical sequences comprise a large fraction of the replication-competent HIV reservoir.** *PLoS Pathog* 2017; **13**:e1006283.
3. Lorenzi JC, Cohen YZ, Cohn LB, Kreider EF, Barton JP, Learn GH, *et al*. **Paired quantitative and qualitative assessment of the replication-competent HIV-1 reservoir and comparison with integrated proviral DNA.** *Proc Natl Acad Sci U S A* 2016; **113**: E7908–E7916.
4. Lee GQ, Orlova-Fink N, Einkauf K, Chowdhury FZ, Sun X, Harrington S, *et al*. **Clonal expansion of genome-intact HIV-1 in functionally polarized Th1 CD4$^+$ T cells.** *J Clin Invest* 2017; **127**:2689–2696.
5. Chomont N, El-Far M, Ancuta P, Trautmann L, Procopio FA, Yassine-Diab B, *et al*. **HIV reservoir size and persistence are driven by T cell survival and homeostatic proliferation.** *Nat Med* 2009; **15**:893–900.
6. Wang Z, Gurule EE, Brennan TP, Gerold JM, Kwon KJ, Hosmane NN, *et al*. **Expanded cellular clones carrying replication-competent HIV-1 persist, wax, and wane.** *Proc Natl Acad Sci U S A* 2018; **115**:E2575–E2584.
7. Douek DC, Brenchley JM, Betts MR, Ambrozak DR, Hill BJ, Okamoto Y, *et al*. **HIV preferentially infects HIV-specific CD4$^+$ T cells.** *Nature* 2002; **417**:95–98.
8. Maldarelli F, Wu X, Su L, Simonetti FR, Shao W, Hill S, *et al*. **HIV latency. Specific HIV integration sites are linked to clonal expansion and persistence of infected cells.** *Science (New York, NY)* 2014; **345**:179–183.
9. Wagner TA, McLaughlin S, Garg K, Cheung CY, Larsen BB, Styrchak S, *et al*. **HIV latency. Proliferation of cells with HIV integrated into cancer genes contributes to persistent infection.** *Science* 2014; **345**:570–573.
10. Wiegand A, Spindler J, Hong FF, Shao W, Cyktor JC, Cillo AR, *et al*. **Single-cell analysis of HIV-1 transcriptional activity reveals expression of proviruses in expanded clones during ART.** *Proc Natl Acad Sci U S A* 2017; **114**:E3659–E3668.
11. Hosmane NN, Kwon KJ, Bruner KM, Capoferri AA, Beg S, Rosenbloom DI, *et al*. **Proliferation of latently infected CD4$^+$ T cells carrying replication-competent HIV-1: potential role in latent reservoir dynamics.** *J Exp Med* 2017; **214**:959–972.
12. Simonetti FR, Sobolewski MD, Fyne E, Shao W, Spindler J, Hattori J, *et al*. **Clonally expanded CD4$^+$ T cells can produce infectious HIV-1 in vivo.** *Proc Natl Acad Sci U S A* 2016; **113**:1883–1888.
13. Kearney MF, Wiegand A, Shao W, Coffin JM, Mellors JW, Lederman M, *et al*. **Origin of rebound plasma HIV includes cells with identical proviruses that are transcriptionally active before stopping of antiretroviral therapy.** *J Virol* 2016; **90**:1369–1376.
14. Roche M, Tumpach C, Symons J, Gartner M, Anderson JL, Khoury G, *et al*. **CXCR4-using HIV strains predominate in naive and central memory CD4$^+$ T cells in people living with HIV on antiretroviral therapy: implications for how latency is established and maintained.** *J Virol* 2019; **4**:e01736-19.
15. Buzon MJ, Sun H, Li C, Shaw A, Seiss K, Ouyang Z, *et al*. **HIV-1 persistence in CD4$^+$ T cells with stem cell-like properties.** *Nature medicine* 2014; **20**:139–142.
16. Zerbato JM, McMahon DK, Sobolewski MD, Mellors JW, Sluis-Cremer N. **Naive CD4$^+$ T cells harbor a large inducible reservoir of latent, replication-competent human immunodeficiency virus type 1.** *Clin Infect Dis* 2019; **69**:1919–1925.
17. Kwon KJ, Timmons AE, Sengupta S, Simonetti FR, Zhang H, Hoh R, *et al*. **Different human resting memory CD4(+) T cell subsets show similar low inducibility of latent HIV-1 proviruses.** *Sci Transl Med* 2020; **12**:eaax6795.
18. Flynn JK, Gorry PR. **Stem memory T cells (TScentral memory)—their role in cancer and HIV immunotherapies.** *Clin Transl Immunol* 2014; **3**:e20.
19. Cashin K, Paukovics G, Jakobsen MR, Østergaard L, Churchill MJ, Gorry PR, Flynn JK. **Differences in coreceptor specificity contribute to alternative tropism of HIV-1 subtype C for CD4 (+) T-cell subsets, including stem cell memory T-cells.** *Retrovirology* 2014; **11**:97.
20. Tabler CO, Lucera MB, Haqqani AA, McDonald DJ, Migueles SA, Connors M, Tilton JC. **CD4(+) memory stem cells are infected by HIV-1 in a manner regulated in part by SAMHD1 expression.** *J Virol* 2014; **88**:4976–4986.
21. Moldt B, Chandrashekar A, Borducchi EN, Nkolola JP, Stephenson H, Nagel M, *et al*. **HIV envelope antibodies and TLR7 agonist partially prevent viral rebound in chronically SHIV-infected monkeys.** *PLoS Pathog* 2022; **18**:e1010467.
22. Sneller MC, Blazkova J, Justement JS, Shi V, Kennedy BD, Gittens K, *et al*. **Combination anti-HIV antibodies provide sustained virological suppression.** *Nature* 2022; **606**:375–381.
23. Niessl J, Baxter AE, Mendoza P, Jankovic M, Cohen YZ, Butler AL, *et al*. **Combination anti-HIV-1 antibody therapy is associated with increased virus-specific T cell immunity.** *Nat Med* 2020; **26**:222–227.
24. Bertagnolli LN, Varriale J, Sweet S, Brockhurst J, Simonetti FR, White J, *et al*. **Autologous IgG antibodies block outgrowth of a substantial but variable fraction of viruses in the latent reservoir for HIV-1.** *Proc Natl Acad Sci U S A* 2020; **117**:32066–32077.

25. Registre L, Moreau Y, Ataca ST, Pulukuri S, Henrich TJ, Lin N, Sagar M. **HIV-1 coreceptor usage and variable loop contact impact V3 loop broadly neutralizing antibody susceptibility.** *J Virol* 2020; **94**:e01604–e01619.
26. Khoury G, Anderson JL, Fromentin R, Hartogenesis W, Smith MZ, Bacchetti P, *et al*. **Persistence of integrated HIV DNA in CXCR3 + CCR6 + memory CD4$^+$ T cells in HIV-infected individuals on antiretroviral therapy.** *AIDS* 2016; **30**:1511–1520.
27. Kumar S, Stecher G, Tamura K. **MEGA7: Molecular Evolutionary Genetics Analysis Version 7.0 for bigger datasets.** *Mol Biol Evol* 2016; **33**:1870–1874.
28. Tamura K, Nei M, Kumar S. **Prospects for inferring very large phylogenies by using the neighbor-joining method.** *Proc Natl Acad Sci U S A* 2004; **101**:11030–11035.
29. Nei M, Kumar S. *Molecular evolution and phylogenetics*. Oxford; New York: Oxford University Press; 2000.
30. Kearney MF, Spindler J, Shao W, Yu S, Anderson EM, O'Shea A, *et al*. **Lack of detectable HIV-1 molecular evolution during suppressive antiretroviral therapy.** *PLoS Pathog* 2014; **10**: e1004010.
31. Wang TH, Donaldson YK, Brettle RP, Bell JE, Simmonds P. **Identification of shared populations of human immunodeficiency virus type 1 infecting microglia and tissue macrophages outside the central nervous system.** *J Virol* 2001; **75**:11686–11699.
32. Gorry PR, Taylor J, Holm GH, Mehle A, Morgan T, Cayabyab M, *et al*. **Increased CCR5 affinity and reduced CCR5/CD4 dependence of a neurovirulent primary human immunodeficiency virus type 1 isolate.** *J Virol* 2002; **76**:6277–6292.
33. Gray L, Sterjovski J, Churchill M, Ellery P, Nasr N, Lewin SR, *et al*. **Uncoupling coreceptor usage of human immunodeficiency virus type 1 (HIV-1) from macrophage tropism reveals biological properties of CCR5-restricted HIV-1 isolates from patients with acquired immunodeficiency syndrome.** *Virology* 2005; **337**:384–398.
34. Gorry PR, Dunfee RL, Mefford ME, Kunstman K, Morgan T, Moore JP, *et al*. **Changes in the V3 region of gp120 contribute to unusually broad coreceptor usage of an HIV-1 isolate from a CCR5 Delta32 heterozygote.** *Virology* 2007; **362**:163–178.
35. Fromentin R, Bakeman W, Lawani MB, Khoury G, Hartogensis W, DaFonseca S, *et al*. **CD4$^+$ T cells expressing PD-1, TIGIT and LAG-3 contribute to HIV persistence during art.** *PLoS Pathog* 2016; **12**:e1005761.
36. Khoury G, Fromentin R, Solomon A, Hartogensis W, Killian M, Hoh R, *et al*. **Human immunodeficiency virus persistence and t-cell activation in blood, rectal, and lymph node tissue in human immunodeficiency virus-infected individuals receiving suppressive antiretroviral therapy.** *J Infect Dis* 2017; **215**:911–919.
37. Salazar-Gonzalez JF, Bailes E, Pham KT, Salazar MG, Guffey MB, Keele BF, *et al*. **Deciphering human immunodeficiency virus type 1 transmission and early envelope diversification by single-genome amplification and sequencing.** *J Virol* 2008; **82**:3952–3970.
38. Yu X, Gilbert PB, Hioe CE, Zolla-Pazner S, Self SG. **Statistical approaches to analyzing HIV-1 neutralizing antibody assay data.** *Stat Biopharm Res* 2012; **4**:1–13.
39. Wagh K, Bhattacharya T, Williamson C, Robles A, Bayne M, Garrity J, *et al*. **Optimal combinations of broadly neutralizing antibodies for prevention and treatment of HIV-1 Clade C infection.** *PLoS Pathog* 2016; **12**:e1005520.
40. McManus WR, Bale MJ, Spindler J, Wiegand A, Musick A, Patro SC, *et al*. **HIV-1 in lymph nodes is maintained by cellular proliferation during antiretroviral therapy.** *J Clin Invest* 2019; **129**:4629–4642.
41. Van Zyl GU, Katusiime MG, Wiegand A, McManus WR, Bale MJ, Halvas EK, *et al*. **No evidence of HIV replication in children on antiretroviral therapy.** *J Clin Invest* 2017; **127**:3827–3834.
42. von Stockenstrom S, Odevall L, Lee E, Sinclair E, Bacchetti P, Killian M, *et al*. **Longitudinal genetic characterization reveals that cell proliferation maintains a persistent HIV type 1 DNA pool during effective HIV therapy.** *J Infect Dis* 2015; **212**:596–607.
43. Wagner TA, McKernan JL, Tobin NH, Tapia KA, Mullins JI, Frenkel LM. **An increasing proportion of monotypic HIV-1 DNA sequences during antiretroviral treatment suggests proliferation of HIV-infected cells.** *J Virol* 2013; **87**:1770–1778.
44. Wibmer CK, Bhiman JN, Gray ES, Tumba N, Abdool Karim SS, Williamson C, *et al*. **Viral escape from HIV-1 neutralizing antibodies drives increased plasma neutralization breadth through sequential recognition of multiple epitopes and immunotypes.** *PLoS Pathog* 2013; **9**:e1003738.
45. Wei X, Decker JM, Wang S, Hui H, Kappes JC, Wu X, *et al*. **Antibody neutralization and escape by HIV-1.** *Nature* 2003; **422**:307–312.
46. Richman DD, Wrin T, Little SJ, Petropoulos CJ. **Rapid evolution of the neutralizing antibody response to HIV type 1 infection.** *Proc Natl Acad Sci U S A* 2003; **100**:4144–4149.
47. Wilson A, Shakhtour L, Ward A, Ren Y, Recary M, Stevenson E, *et al*. **Characterizing the relationship between neutralization sensitivity and env gene diversity during ART suppression.** *Front Immunol* 2021; **12**:710327.
48. Bunnik EM, Quakkelaar ED, van Nuenen AC, Boeser-Nunnink B, Schuitemaker H. **Increased neutralization sensitivity of recently emerged CXCR4-using human immunodeficiency virus type 1 strains compared to coexisting CCR5-using variants from the same patient.** *J Virol* 2007; **81**:525–531.
49. Ren Y, Korom M, Truong R, Chan D, Huang SH, Kovacs CC, *et al*. **Susceptibility to neutralization by broadly neutralizing antibodies generally correlates with infected cell binding for a panel of Clade B HIV reactivated from latent reservoirs.** *J Virol* 2018; **92**:e00895–e00818.
50. Bruner KM, Murray AJ, Pollack RA, Soliman MG, Laskey SB, Capoferri AA, *et al*. **Defective proviruses rapidly accumulate during acute HIV-1 infection.** *Nat Med* 2016; **22**:1043–1049.
51. Hiener B, Horsburgh BA, Eden JS, Barton K, Schlub TE, Lee E, *et al*. **Identification of genetically intact HIV-1 proviruses in specific CD4(+) T cells from effectively treated participants.** *Cell Rep* 2017; **21**:813–22.
52. Cohen YZ, Lorenzi JCC, Seaman MS, Nogueira L, Schoofs T, Krassnig L, *et al*. **Neutralizing activity of broadly neutralizing anti-HIV-1 antibodies against Clade B clinical isolates produced in peripheral blood mononuclear cells.** *J Virol* 2018; **92**:e01883-17.
53. Provine NM, Cortez V, Chohan V, Overbaugh J. **The neutralization sensitivity of viruses representing human immunodeficiency virus type 1 variants of diverse subtypes from early in infection is dependent on producer cell, as well as characteristics of the specific antibody and envelope variant.** *Virology* 2012; **427**:25–33.